Subsonic Flow Visualization Using Steam

C. J. PRENTICE* AND F. X. HURLEY†
McDonnell Douglas Corporation, St. Louis, Mo.

THERE exists a variety of streamline tracing techniques for flowfield study in the low subsonic speed regime.[1] At moderately fast subsonic speeds (i.e., over 200 fps), it is rather difficult to produce a sufficiently dense "smoke," although certain oil vapor generators have achieved this capability.[2] The purpose of this Note is to draw attention to a simple method of streamline tracing above 200 fps which does not require any special chemicals or mechanical or heating equipment.

A standard method of supersonic flow visualization is the vapor screen technique[3] wherein the working gas is moistened at some point upstream. Upon isentropic expansion through the supersonic nozzle, the gas experiences a temperature drop, and it surrenders some of its moisture as a fog of water droplets which when properly illuminated reveals the details of the flow. It seems reasonable that the same principle should work in a subsonic tunnel if steam accompanied by a cooling agent from an external source is introduced into the flowfield. Preliminary tests discussed below have shown that a mixture of steam and cold nitrogen gas produces a streamline-tracing fog which is persistently visible.

Saturated steam was tapped from the building supply line at a nominal gage pressure of 25 lb/in^2. The source of nitrogen gas was a standard 110 l liquid nitrogen Dewar at 23 lb/in.^{2} gage. Fifteen-foot lengths of $\frac{1}{2}$-in. hydraulic hose and $\frac{1}{4}$-in. copper tubing carried, respectively, the steam and the nitrogen into the tunnel where they were allowed to mix annularly at a point 1-ft upstream of the model being tested.

Uncalibrated valves at both the steam and nitrogen sources were used to control the mass flows of each component. The "best" valve settings depend in a complex manner on tunnel speed and test setup, but it was not difficult to achieve the preferred balance through trial and error adjustment during the run. Also it is noted that several minutes were required for the steam hose to reach a sufficiently high temperature so that the steam was not condensed before reaching the test section.

Figure 1 illustrates stream tube marking by the steam plus nitrogen mixture in the McDonnell Low Speed Wind Tunnel at a flow velocity of 250 fps. The high aspect ratio airfoil model has a chord of 9 in. The flow visualization effect was improving somewhat with speed at this point for the relative spreading of the fog lessens with speed. The photograph presents the effect as it was seen by observers during the event; normal tunnel lighting was used, and no special film or time exposure was employed.

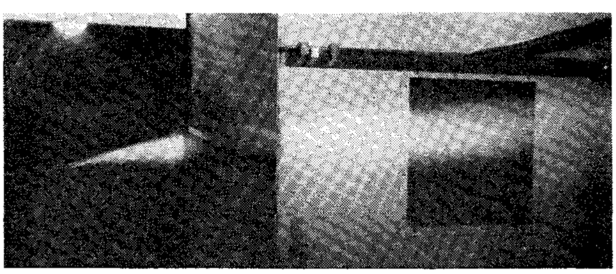

Fig. 1 Fog produced by a mixture of steam and cold nitrogen gas in a 250-fps airflow over a 9-in. chord airfoil model.

Received February 2, 1970. This work was conducted under the McDonnell Douglas Independent Research and Development program.

* Senior Engineer, Gas Dynamics Laboratory, McDonnell Aircraft Company.

† Research Scientist, Fluid Mechanics Group, McDonnell Douglas Research Laboratories. Member AIAA.

References

[1] Maltby, R. L. and Keating, R. F. A., "Smoke Techniques for Use in Low Speed Wind Tunnels," AGARDograph 70, Pt. III, April 1962, NATO.

[2] Sellberg, L. D., "Smoke Generator Type Lorinder for Flow Visualization in Low Speed Wind Tunnels," KTH-AERO-TN-55, June 1966, (Swedish) Royal Institute of Technology.

[3] McGregor, I., "Development of the Vapor Screen Method of Flow Visualization in a Three-Foot Supersonic Wind Tunnel," AGARDograph 70, Pt. IV, April 1962, NATO.

Test Section for a V/STOL Wind Tunnel

CHING-FANG LO*
ARO Inc., Arnold Air Force Station, Tenn.

Introduction

IT has been recognized[1] that a wind tunnel with ventilated walls offers promise as a configuration for V/STOL testing in an acceptable environment. Among some previous investigations, Wright[2] suggests a test section with a solid upper wall, slotted vertical walls, and an open lower boundary for small interference. The drawback of the open lower boundary is that it may introduce oscillations of the test section flow; however, these oscillations could be removed by replacing the open lower boundary with a many slotted boundary as suggested in Ref. 2. A closed-on-bottom-only configuration with a selected height-to-width ratio for each wake angle is suggested by Heyson[3] but poses many related practical problems in designing the wind tunnel.

A test section having solid vertical and slotted horizontal walls with equal porosity has been studied by the author.[4] The value of slot opening which results in zero interference has been found as a function of model wake angle. However, since the proper value of slot opening is a function of wake angle, it seems that one more variable is needed to achieve a configuration yielding zero upwash interference for all wake angles. Hence, a test section with solid vertical walls and different porosities for the top and bottom walls has been chosen for the present study. This did result in a configuration which gives nearly zero interference at the model position for every wake angle. The interference distributions along the streamwise and spanwise directions were determined for this selected configuration.

Analysis

The field equation of an inviscid, irrotational fluid for incompressible flow in terms of the perturbation velocity potential φ in Cartesian coordinates (Fig. 1) is

$$(\partial^2\varphi/\partial x^2) + (\partial^2\varphi/\partial y^2) + (\partial^2\varphi/\partial z^2) = 0 \qquad (1)$$

The boundary conditions for a tunnel consisting of solid vertical walls and slotted horizontal walls with different

Received April 1, 1970. The research reported herein was sponsored by the Arnold Engineering Development Center, Air Force Systems Command, under Contract No. F-40600-69-C0001 S/A 10(70) with ARO Inc. Further reproduction is authorized to satisfy needs of the U.S. Government.

* Research Engineer, Propulsion Wind Tunnel Facility. Member AIAA.

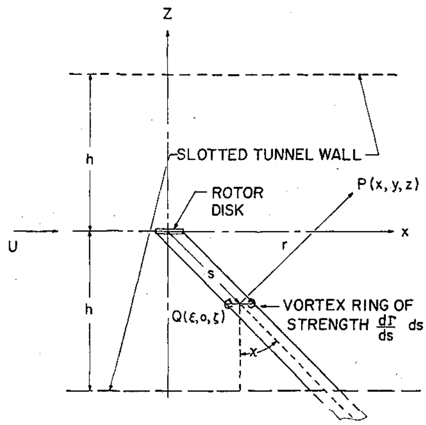

Fig. 1 Mathematical representation of a V/STOL model in a slotted wind tunnel.

porosities are expressed as

$$(\partial\varphi/\partial y) = 0 \qquad \text{at } y = \pm b \tag{2}$$

$$\varphi + K_t(\partial\varphi/\partial z) = 0 \qquad \text{at } z = h$$
$$\varphi - K_b(\partial\varphi/\partial z) = 0 \qquad \text{at } z = -h \tag{3}$$

where K is related to the open area ratio a/l as $K = (l/\pi)\ln[\csc(\pi a/2l)]$. The slot parameter is introduced as $P = [(1 + (K/h)]^{-1}$ where the value of $P = 0$ corresponds to a closed wall and $P = 1$ to an open wall. The subscript t and b denote the top and bottom walls, respectively.

The linearity of the field equation and its boundary condition permits the perturbation potential to be separated into two parts as $\varphi = \varphi_m + \varphi_i$ where φ_m is the disturbance potential due to the model in free air and φ_i is the interference potential induced by the tunnel walls.

The disturbance potential of a rotor, lifting fan, or lifting jet is represented[2,4] by an elliptic vortex cylinder sheet. The model is assumed to be mounted at the center of the test section and the vortex cylinder is swept downstream by a skew angle χ for zero angle of attack as shown in Fig. 1. The zero angle of attack is chosen for simplicity, since the interference is a weak function of the angle of attack.[3,4] The vortex sheet is made up of a continuous constant-strength distribution of circular vortex rings lying in planes parallel to the rotor plane. Under the small model assumption, the

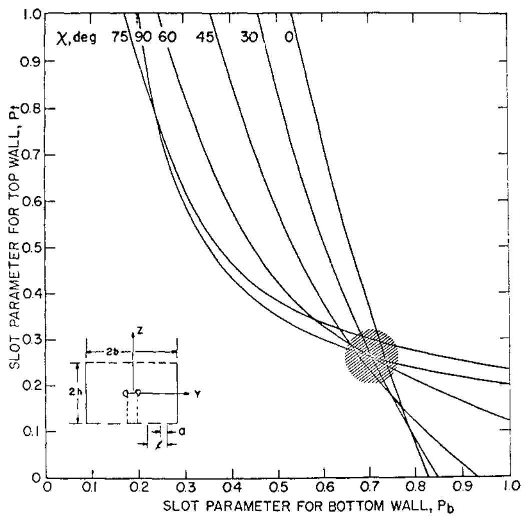

Fig. 2 Zero interference curves with solid vertical walls and top and bottom walls of various porosities for h/b = 0.667.

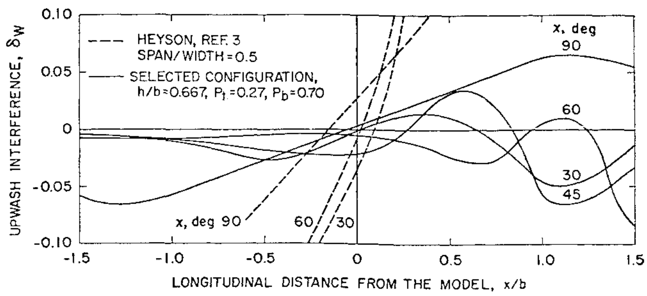

Fig. 3 Longitudinal distribution of interference for a small model in a slotted tunnel and for a finite model in Heyson's scheduled variable height-to-width, closed-on-bottom only tunnels.

disturbance potential may be obtained by summing up each vortex ring along the assumed straight wake path from the rotor to the wake-wall intersection point, which is the primary portion contributing to the interference. The expression for the disturbance is of the form

$$\varphi_m = \int d\varphi_m = \int_0^{s_0} A\,\frac{d\Gamma}{ds}\,\frac{(z+\zeta)}{4\pi r^3}\,ds \tag{4}$$

where $r = |PQ| = [(x-\xi)^2 + y^2 + (z+\zeta)^2]^{1/2}$, A = cross-sectional area of rotor.

The method used to obtain the interference potential, φ_i, from Eqs. (1–3) is the image method in conjunction with Fourier transforms. An image system, which consists of a row of images is introduced to satisfy Eq. (2) on the solid vertical walls. Fourier transforms are then used to solve Eq. (1) and its associated boundary conditions Eq. (3). This yields the interference potential, hence, the upwash and streamwise interference components. The method is fully described in Ref. 4.

Selection of Test Section Configuration

The criterion used to select a combination of top and bottom wall porosities is based on zero or near zero upwash interference, since the wall correction is dominated by the upwash component which is expressed as

$$\delta_w = \frac{\text{area of test section}}{\text{area of rotor disk}}\,\frac{1}{\frac{1}{2}(d\Gamma/ds)}\left(\frac{\partial\varphi_i}{\partial z}\right) \tag{5}$$

The combination of top and bottom wall porosities which give zero upwash interference for various skew angles, are shown in Fig. 2. A striking result from Fig. 2 is that the curve for each different skew angle crosses a small region indicated by the shaded area. This implies that a configuration with a porosity combination inside the shaded area of Fig. 2 will give zero or near zero interference for each skew angle.

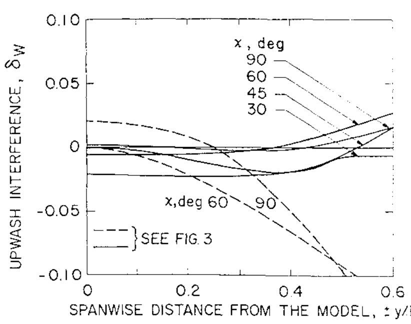

Fig. 4 Lateral distribution of interference for a small model in a slotted tunnel and for a finite model in Heyson's scheduled variable height-to-width closed-on-bottom only tunnels.

The longitudinal and lateral distributions of interference for such a configuration, $P_t = 0.27$ and $P_b = 0.70$, are plotted in Figs. 3 and 4. These curves indicate that the upwash interference is reduced to practically zero in both the streamwise and spanwise direction from the model. Some results[3] of a finite span model in the scheduled height-to-width closed-on-bottom tunnels are shown in Figs. 3 and 4 for comparison purposes.

In conclusion, a selected single configuration was obtained which eliminates interferences, in the streamwise and spanwise direction simultaneously, for all rotor wake skew angles.

References

[1] Lo, C. F. and Binion, T. W., Jr., "A V/STOL Wind Tunnel Interference Study," *Journal of Aircraft*, Vol. 7, No. 1, Jan.-Feb., 1970, pp. 51–57.

[2] Wright, R. H. "Test Sections for Small Theoretical Wind Tunnel Boundary Interference on V/STOL Models," TR-R-286, 1968, NASA.

[3] Heyson, H. H. "Theoretical Study of the Use of Variable Geometry in the Design of Minimal-Correction V/STOL Wind Tunnels," TR R-318, 1969, NASA.

[4] Lo, C. F. "Wind Tunnel Boundary Interference on a V/STOL Model," AIAA Paper 70-575, Tullahoma, Tenn., May, 1970.

A Rapid Method for Flow Splitter Design in 3-D Exhaust Nozzles

A. M. Bloom*

McDonnell Douglas Corporation, Long Beach, Calif.

Nomenclature

A = flow area
H = flow height
l = circular arc length
L = nozzle length
m = number of channels
M = Mach number
p = pressure
r = radial coordinate
T = temperature
W = flow width
z = axial coordinate
α = area fraction
ρ = mass density
ϕ = circumferential coordinate

Subscripts

B = bifurcation
I = inner
j = circumferential boundary index
k = axial coordinate index
L = lower
M = mean
O = outer
s = stagnation
T = total
U = upper

Superscripts

j = jth circumferential boundary

I. Introduction

The design of flow splitters in exhaust nozzles is a problem which arises in the design of transport jet engines that cruise at high subsonic Mach numbers. Flow splitters are included in exhaust nozzles to provide surface area for acoustical treatment and to reduce swirl. Hence, the annular passage of the exhaust nozzle is divided into a number of circumferential channels by radial splitters. The design problem consists of determining the splitter locations such that the individual channels have similar flow distributions. The approach of the present design method is to compute the flow area distribution in each channel by a three-dimensional flow area approximation. Then, based on the assumption of a one-dimensional steady compressible inviscid flow, the corresponding Mach number distributions are obtained in each channel. The channel walls are constructed in such a manner that the one-dimensional Mach number distributions in each channel are identical. The present design method is easily programed on a digital computer and has been found to be quite useful for radial splitter design in fan exhaust nozzles used in high-bypass-ratio jet engines.

In this paper, a design method for flow splitters in three-dimensional fan exhaust nozzles is presented. The nozzle contours are represented by surfaces of revolution, and the flow passage is divided into a given number of channels by radial splitters. The basic assumption of the present design method is that the flowfield in each channel of the exhaust nozzle can be considered as a one-dimensional steady compressible flow. Then, based on the conformal representation of an arbitrary surface of revolution by a right circular cylinder[1] an approximation for the channel flow area distributions can be computed in order to represent the nozzle flowfield by one-dimensional equations. A similar idea for the calculation of flow area was proposed by Pratt and Whitney[2]; however, their procedure was graphical in nature. The design problem envolves determining the circumferential position of the radial flow splitters in such a manner that the Mach number distributions in each of the channels are identical.

Received January 15, 1970.

* Engineer/Scientist Specialist, Power Plant Group, Douglas Aircraft Division. Member AIAA.

II. Nozzle Geometry

A cylindrical coordinate system (r,ϕ,z) is taken to describe the fan exhaust nozzle (Fig. 1). The upper and lower pylon that bifurcate the nozzle are accounted for by defining so called upper and lower bifurcation angles ϕ_U and ϕ_L, whose variation with the z coordinate is assumed to be given. Hence, the region available for mass flow consists of two symmetric channels. Therefore, it is sufficient to consider the region defined by

$$r_I(z) \leq r \leq r_0(z)$$
$$\phi_L(z) \leq \phi \leq \pi - \phi_U(z) \qquad (1)$$
$$0 \leq z \leq L$$

If the region defined by Eq. (1) is divided into m channels by $(m - 1)$ radial splitters, the angles $\phi_j(z)$, $j = 1,2, \ldots,$ $m + 1$ define the circumferential channel boundaries (Fig. 1).

III. Flow Area Approximation

The definition of flow area in the jth channel is based on the concepts of a flow width $W_j(z)$ and a flow height $H(z)$. If the mean radius distribution is defined by the arithmetic mean

$$r_M(z) = \tfrac{1}{2}[r_I(z) + r_0(z)], \; 0 \leq z \leq L \qquad (2)$$

then the flow height is defined by

$$H(z) = [r_0(z) - r_I(z)] \cdot \cos[\tan^{-1}(r'_M)] \qquad (3)$$

where the prime denotes differentiation with respect to z. It should be noted that the mean radius distribution introduced in Eq. (2) defines a mean surface of revolution $[r_M(z),$ $\phi,z]$. Hence, the flow area in the jth channel is expressed by

$$A_j(z) = W_j(z) \cdot H(z), \; j = 1,2, \ldots, m \qquad (4)$$

The flow width $W_j(z)$ in the jth channel is defined as an arc